EFFECTS OF TARGET PROPERTIES ON CRATER SIZES AND ITS IMPLICATIONS ON AGE DETERMINATION - INSIGHTS FROM NUMERICAL EXPERIMENTS

N. C. Prieur[1], Z. Xiao[1,3,4], K. Wünnemann[2] and S. C. Werner[1]. [1]Centre for Earth Evolution and Dynamics, University of Oslo, Norway, [2]Museum für Naturkunde, Leibniz-Institute for Evolution and Biodiversity Science, Berlin, Germany, [3]Planetary Science Institute, China University of Geosciences, 430074 Wuhan, Hubei, PR China, [4]Space Science Institute, Macau University of Science and Technology (contact: nilscp@geo.uio.no).

Introduction: The size-dependent crater density is commonly used to determine relative sequences of geological events. For a given chronology model, these relative ages can be used to derive ages of geological units on a planetary surface [1]. For geologically young features on planetary surfaces, only small craters are available to derive an age [2, 3]. At these sizes (D<~1 km), cratering occurs in both strength-and gravity-regimes. Numerical simulations and observations have shown that for given impact energy the diameter of the resulting impact crater depends on the target strength [e.g., 4, 5]. Consequently, the crater-projectile size relation is ambiguous due to target properties, which challenges the crater-based age determination, if the underlying chronology model and crater production functions are derived and applied on differing target types. Thus, in this case, the age derived may be erroneous.

Discrepancies in ages derived on impact melts and ejecta for Copernican-aged craters (i.e., young lunar craters) are thought to be a consequence of different target properties [e.g., 6–8] and self-secondaries [e.g., 9–11]. However, quantification of the role of target properties in crater formation and their influence on the crater size-frequency distribution (SFD) are still under debate and a clear understanding of these effects are missing [3, 7]. Earlier studies investigating these problems [e.g., 7, 12, 13] used common crater scaling laws [14] in order to quantify the effect of target properties on the age determination. However, such scaling laws only predict the size of the transient crater on a homogeneous target and apply a constant factor to relate transient and final crater diameters [e.g., 8, 12, 13], thus omitting the possible dependence of the degree of collapse on target properties.

In this study, we develop new scaling laws for brecciated and competent materials from systematic numerical experiments ([4, 15], see Table 1). The new relations are then used to derive target depending crater size – projectile size scaling laws. These new relations are then applied to measurements on melt pool and ejecta units of the Tycho crater.

Methods: In this work, we use the shock physics code iSALE [16–18]. We modeled vertical (90°) impacts with an impact velocity of 12.7 km/s (which corresponds to the vertical component of the most likely impact velocity 18 km/s at a 45° angle on the Moon). Projectile diameters are varied over a wide range (0.1–100 m) to cover both craters formed in the strength- and in the gravity-dominated regime. Target parameters such as porosity, friction and cohesive strength are varied over a range of plausible values for lunar materials [19–21] to study their effects on the crater-size frequency distribution slope, looking for potential systematic diameter shifts. We account for differences in porosity and material strength in the two target types by using a porosity compaction model [20] and the Drucker-Prager strength model (for all models except model names in bold). In all models, the projectile consists of non-porous basalt, which is the same material used to model the lunar surface. A resolution of 10 cells per projectile radius (CPPR) has been selected to achieve a good compromise between a small relative error on the crater diameter (10%) and a feasible computational time.

In order to investigate the effect of target properties on the age derived from crater counting, the final crater diameter needs to be determined. The transient crater is measured at the time when the crater volume reaches its first local maximum [15]. In addition, several simulations were run until crater completion to get a relationship between the transient crater and the final rim-rim crater diameter. Crater counts on the melt pool and ejecta units of Tycho were collected (see [22]).

Table 1 *Target properties tested in this study. IM and EJ stand for Impact Melt and Ejecta, respectively.*

Models	Friction	Porosity	Cohesion
IM1	0.8	20 %	0.1 MPa
IM2	0.8	10 %	0.5 MPa
IM3*	0.6	12 %	1.0 MPa
EJ1	0.6	50 %	0 MPa
EJ2	0.8	20 %	0 MPa
EJ3*	0.6	15 %	0MPa
EJ4	0.8	20 %	0.1 MPa

** models with a resolution of 20 CPPR and a different strength/damage model (see [20]).*

Discussion: Our new scaling laws are presented in Figure 1. The crater-size frequency distributions observed on Tycho's units with different strengths are presented in Figure 2A. The impactor size-frequency

distributions (ISFDs) derived from our scaling laws and measured crater frequencies, correcting for target-properties differences, is presented in Figure 2B.

If target properties are the main factor for the derived age discrepancies, some parts (or even the entire) projectile SFDs should overlap. According to the results presented here, changes in target properties can explain some age discrepancies found at Tycho crater (see Table 1 and Figure 2B). As an example, a strength contrast between EJ4 (0.1 MPa) and EJ2 (0 MPa) may lead to 5-10 times higher impactor frequencies (Figure 2B), whereas, in other cases, a change in combination of target parameters cause a smaller shift of the ISFDs (IM1/IM2 & EJ1/EJ2). Thus, a more systematic and comprehensive analysis of the influence of target parameters on the derived ISFDs is required in order to see if certain combinations of target properties could result in an overlap of the ISFDs derived from the impact melt and ejecta units.

Conclusion: Preliminary results suggest that we can use the already developed tools to shed new light on the influence of target properties on age determination. However, it is already clear that not the entire range of the projectile size-frequency distribution can be fitted. Therefore, we will address contributions of secondary cratering as an additional complication in our future attempts. In addition, target properties will be further tested against the observations on the relevant units of Tycho. We will also consider the variation of target properties with depth; moreover, multi-layered targets will be included in our simulations to model a more realistic lunar surface [e.g., 23].

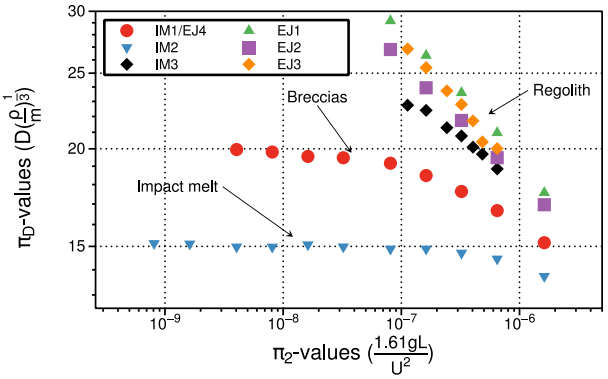

Figure 1 *Comparison of the crater-projectile relation for projectile sizes on various targets (incompetent and competent rocks).*

Acknowledgements: NCP, ZX and SCW appreciated the support by the Research Council of Norway (235058/F20 CRATER CLOCK) and IS-DAAD mobility grant (NFR 244761/F11). KW is supported by the IS DAAD mobility grant 57159947. We would like to acknowledge the developers of iSALE, including Gareth Collins, Dirk Elbeshausen, Boris Ivanov and Jay Melosh. We would also like to thank Tom Davison for the pySALEPlot tool which was used in this work.

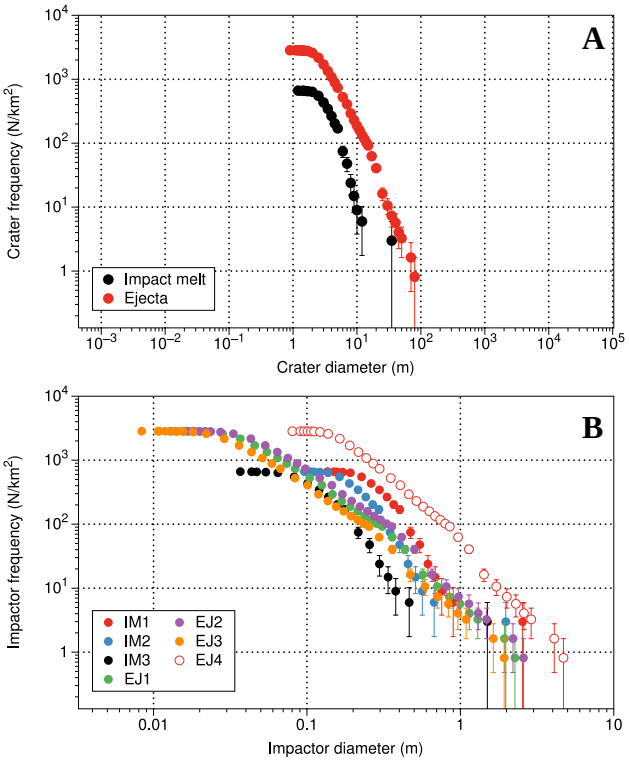

Figure 2 (A) *Cumulative crater size frequency distribution as measured on the melt pools and ejecta blanket of Tycho. At first impression, both crater distributions look different.* **(B)** *Cumulative projectile size frequency distribution recalculated with the appropriate crater to projectile scaling. Curves were derived from crater-size frequency distributions on impact melt (IM) and ejecta (EJ) units (Figure 2A) with scaling laws in Figure 1.*

References: [1] McGill (1977) Geol. Soc. of America, 8, 1102-1110. [2] Williams & Pathare (2015) Workshop on Issues in Craters Studies, Abstract #9051. [3] Werner & Ivanov (2015) Treatise on Geophysics chapter 10-10, 327-365. [4] Wünnemann et al. (2010) Proc. 11th HVIS, 120. [5] Schultz & Spencer (1979) LPSC 10, 1081-1083. [6] van der Bogert et al. (2010) LPSC 41, #2165. [7] Hiesinger et al. (2012) JGR 117, E00H10. [8] van der Bogert et al. (2013) LPSC 44, #1962. [9] Shoemaker et al. (1968) in Surveyor VII Mission Report Part II. NASA Tech Rept 32-1265, 9. [10] Plescia et al. (2010) LPSC 41, #2038. [11] Xiao et al. (2016) LPSC, this conference. [12] Dundas et al. (2010) GRL 37, L12203. [13] Kirchoff et al. (2015) LPSC 46, #2121. [14] Holsapple (1993) Annu. Rev. Planet. Sci. 12, 333-373. [15] Elbeshausen et al. (2009) Icarus. 716-731. [16] Amsden et al. (1980) Los Alamos National Report, LA-8095, 0-101. [17] Collins et al. (2004) MAPS, 39, 2, 217-231. [18] Wünnemann et al. (2006) Icarus, 180, 514-527. [19] Slyuta (2014) Sol. Syst. Res., 48, 330-353 [20] Carrier III et al. (1991) Lunar Sourcebook, Chapter 9. [21] Kiefer et al. (2012) GRL, 39, L070201. [22] Xiao & Werner (2015) JGR. [23] K. Wünnemann et al. (2012) LPSC 43, #1805.